20

Low Frequency Noise as a Tool for OCDs Reliability Screening

Qiuzhan Zhou, Jian Gao and Dan'e Wu
Jilin University
China

1. Introduction

With the rapid development of the information and science, more and more newly semiconductor devices are used in the electronic equipments or systems, and so is the Optoelectronic Coupled Devices (OCDs). Because of excellent characteristics of it such as small size, long life, non-contact mode and strong anti-interference, OCDs can replace many kinds of devices e.g. relays, transformers, choppers when used in switching circuits, A/D conversion, remote transmission, over-current protection and so on. The reliability of OCDs is very important in numerous applications. It has draw great attention in switching circuit, isolation circuit, analog-digital converter, logic circuit, etc.
However in some high reliability fields, such as navigation and communication of the satellite, it is necessary to make sure of the reliability of the OCDs. In the past, the reliability screening of the OCDs contained ageing experiments; physical analysis at high and low temperature as well as static testing which are either expensive, time-consuming or cannot separate the good ones from the bad ones. So some researchers proposed that using low frequency noise as a reliability indicator.
From the ninety of the last century, we do the research of using noise as reliability screening of the OCDs and improve it continually. So in this paper, we will introduce how to use low frequency noise as a tool for OCDs reliability screening, and summarize what all we had done as well as the latest research.

2. Analysis of noise types in OCDs

Noise as a diagnostic tool for quality control and reliability estimation of semiconductor devices has been widely accepted and used, and there are many papers published in this area. It is very useful to describe the judging rules, which enable us to predict the individual quality of electronic components, based on measurements of their noise.
It is known that an OCD is made of two parts: LED and Photo detector, both of which are p-n junction devices. So it can be concluded that the noise in OCDs below 1 MHz mainly consists of shot noise, 1/f noise, generation-recombination noise and burst noise. Among them, shot noise and 1/f noise are fundamental. It should be noted that the noise that we are interested in here has strong relation to some typical defects in a device. For this reason, it is necessary that the generation mechanisms of 1/f noise, g-r noise and burst noise in OCDs are all briefly discussed, especially on what kinds of defects can lead to these three kinds of noises. And the relation between them should be discussed as well.

2.1 1/f noise

1/f noise spectrum is inversely proportional to frequency in a very wide range. In homogeneous semiconductors, its spectrum can be characterized by a parameter α according to

$$\frac{S_R}{R^2} = \frac{a}{f_N} \tag{1}$$

where S_R is the power spectral density of the noise in the resistance R, N is the total number of free charge carriers, and f is the measurement spot frequency. The parameter α then is the contribution of one electron to the relative noise at 1 Hz, assuming that the N electrons are uncorrelated noise sources.

In addition, it has been found that α is not a constant, whose value is between 10^{-6} and 10^{-3}, but that α depends on the prevailing type of scattering of the electrons and perfection of the crystal lattice. In recent years much progress has been made and found that it is mainly caused by lattice scattering.

Vandamme has shown that the 1/f noise parameter a increases with the concentration of dislocations and its noise spectrum is proportional to a and inversely proportional to the carrier lifetime. Konczakowska research has indicated that there is a strong relation between bipolar device lifetime and 1/f noise.

Usually 1/f noise in a semiconductor device usually can be divided into fundamental 1/f noise and non-fundamental (or excess) 1/f noise. The fundamental 1/f noise is connected with phenomena which are included in the process of the operation of the electronic component. It is believed that this 1/f noise has no relation to the semiconductor surface and the defects in the bulk.

The 1/f noise which is related to device defects is called non-fundamental 1/f noise, which means that this kind of 1/f noise is caused by device surface or bulk defects in most cases. Thus, it is possible for us to evaluate the device quality and reliability according to its magnitude. From this point of view, non-fundamental 1/f noise is of great value to device quality evaluation and reliability prediction. Most of the evidence suggests that in some types of device it is a surface effect, as in the case of a MOSFET where the semiconductor/oxide interface plays an important role, but in other devices, such as a homogeneous resistor, 1/f noise is thought to be a bulk effect associated with a random modulation of the resistance, implying a fluctuation in either the number or the mobility of the charge carriers. For example, M. Mihaila et al have shown that 1/f noise in a specimen with more dislocations is at least one order of magnitude larger than that of the specimen with fewer dislocations.

Different causes for 1/f noise generation have been reported as follows: (1) the fluctuation of surface recombination velocity in the p-n junction, (2) the fluctuation of trapping in the oxide layer in BJTs or in MOSFETs, (3) dislocation 1/f noise, (4) quantum 1/f noise (in dispute). It is obvious that 1/f noise intensity is related to the generation-recombination center (surface defect) numbers in device oxide layer. Thus, the establishment of a relationship between device surface quality and reliability can help us judge and screen devices according to excess noise intensity.

Therefore it is possible for us to evaluate the device quality and reliability according to its magnitude. From this point of view, 1/f noise is of great value to device quality evaluation and reliability prediction. It is verified that crystal defects cause 1/f noise to increase. The

experimental results have proved that 1/f noise in the specimen with more dislocation is at least one order of magnitude larger than that of the specimen with fewer dislocations.
At present, a major cause of 1/f noise in semiconductor devices is traceable to properties of the surface of the material. The generation and recombination of carriers in surface energy states and density of surface states are important factors, but even the interfaces between silicon surfaces and grown oxide passivation are centers of noise generation. It is obvious that 1/f noise intensity has a relation to the generation-recombination center (surface defect) numbers in device oxide layer. Thus, the relation between device surface quality and 1/f noise is closely related and can be used to screen poor quality devices according to their intensity of excess noise.

2.2 g-r noise

Generation-recombination (g-r) noise distribution is Gaussian and its signal spectrum can be expressed as Lorentzian,

$$\frac{S_R}{R^2} = \frac{S_V}{V^2} = \frac{S_I}{I^2} = \frac{A\tau_0}{1+(\omega\tau_0)^2} \tag{2}$$

Here, $\tau_0=1/\omega_0$ is the characteristic time corresponding to a characteristic (or corner) frequency f_0 or ω_0, and $\omega_0=2\pi f$ is the angular frequency of measurement. g-r noise has a Gaussian amplitude distribution function because it is actually made up from the superposition of a very large number of independent random telegraph signal processes with the same characteristic time. The coefficient, A, is a measure of the number of such individual processes. It depends on g-r center density, current and device structures.
It has been found experimentally that g-r noise is often absent in high quality silicon devices, but not yet in heterostructures, where lattice defects are often a problem. In poor quality devices, the g-r noise is generated at the contacts or at the surface. In better samples, the dominant conductance noise source is in the bulk. Hence, g-r noise used as a useful diagnostic tool to study trap centers in compound semiconductors, is indispensable.
By experimentation it has been shown that the defects (dislocation, deep-level impurities) in the emitter junction and surface are the main g-r noise sources of transistor, especially as a p-n junction is in a forward biased state. Jevtic and Lazovic have shown that excess g-r noise in reverse biased p-n junctions can be caused by g-r centers near the metallurgical junction. These centers may be the impurity in metal clusters associated with dislocations.
Thus, it can be seen that g-r noise in a device has a direct relation to semiconductor defects (impurities, damage etc.). Therefore, it has become an effective method of analyzing bulk defects and reliability screening by means of measuring g-r noise in devices.

2.3 Burst noise

A random telegraph signal (RTS) known as burst noise, is often observed in p-n junction devices such as diodes, transistors and detectors operating under forward biased conditions. All authors have attributed the phenomenon to defects located in the neighborhood of the emitter base junction.
Hsu et al. first presented a physical model of explaining burst noise. In this model, it is thought that heavy metal impurities deposited in the charge region of p-n junction is the major cause of this noise.

But Blasquez has found that so-called ``pure'' lattice dislocation can also cause burst noise even when heavy metal impurity deposits have been removed. Therefore it seems that metal impurity precipitates are not indispensable to produce burst noise. Dai et al. has proposed a new burst model, which emphasizes the built-in electric field in the p-n junction and the variation of the potential barrier near the defects. This model not only is consistent with the experimental results given by Blasquez, but also can explain various burst noise waveforms. In addition, Jevtic has also presented a new physical model of noise sources, which is based on the assumptions that a conduction channel (p-inversion layer) exists in degraded p-n junctions and that the current flow through the defects is modulated by traps adjacent to the defects. The model explains the appearance of two polarity and multi-level pulse noise. Although burst noise spectrum is not Gaussian as are the other types of noise, its current noise spectrum has the shape of Lorentzian,

$$S_I(f) = \frac{A_b \tau_b^2}{1 + \omega^2 \tau_b^2} \tag{3}$$

Where A_b is a constant depending on the nature of the defects and τ_b is defined as $1/\tau_b = 1/\tau_1 + 1/\tau_2$. According to the random switch mode, during the time interval dt, an open switch has the probability dt/τ_1 of closing, and a closed switch a probability dt/τ_2 of opening. The information on the defects is contained in the parameter A_b and τ_b.

Besides, burst (or RTS) noise is a problem typical for submicron MOST's or bipolar devices with crystallographic damage in sensitive areas and this noise is also temperature and bias dependent. Many experiments have already shown that lattice dislocation, a serious defect, is the major source of burst noise for both bipolar transistor and integrated circuit. Therefore, devices with burst noise often degrade faster and at least show a poor noise behavior. Fig. 1 shows a noise waveform of time-domain in an OCD with excess noise.

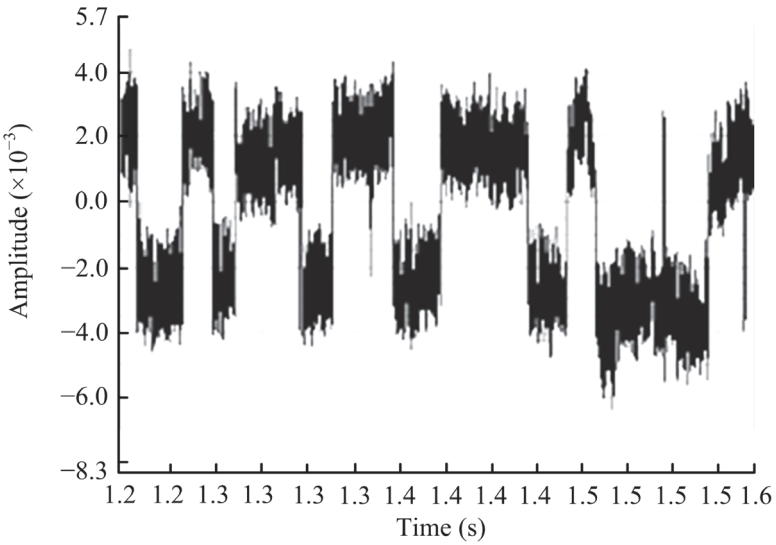

Fig. 1. Noise waveform of time-domain in an OCD with excess noise.

2.4 Brief summary

It can be seen that 1/f noise, g-r noise and burst noise are closely related with some defects such as surface defects, impurities and dislocations, etc. Dislocations and electromigration in metallization affect device reliability, and has been identified as the main source of device failure. Thus, it can be said that 1/f noise is closely related to the surface states of the semiconductor device, g-r noise related to device bulk defects such as impurities, dislocation, etc., and burst noise related to lattice dislocation as well as heavy metal impurity deposits. Besides, emitter region edge dislocation makes both 1/f noise and burst noise increase at the same time in most cases. Strasilla and Struut demonstrated that experimentally observed burst noise consist of a random telegraph signal superimposed on 1/f noise, but the two processes were statistically independent.

Hence in order to exclude these defects and meet high reliability, we can use the three independent noise, 1/f, g-r and burst noise, as reliability indicator for quality estimation of OCDs.

3. The noise measurement and analysis of OCDs

Harder C et al have presented that the noise equivalent circuit of a semiconductor laser diode from the rate equations including Langevin noise sources. This equivalent circuit allows a straightforward calculation of the noise performance of a laser diode combined with extrinsic elements, such as the driving source and the parasitic elements. Recently, using this rate equation, these intrinsic intensity fluctuations in semiconductor laser diode (LD), optoelectronic integrated device (OEID) made by heterojunction phototransistor (HPT) and laser diodes have been analyzed, then the relative intensity noise (RIN) and the correlation between the terminal electrical noise and output optical photocurrent noise have been investigated.

At present, the key to design of low-frequency low noise devices and circuits lies in reducing level of white noise and corner frequency of l/f noise, which has been realized gradually and Whether voltage noise or current noise takes these two parameters as its characteristics. But the present noise measuring apparatus, such as QuanTech2173c/2181 and HP-4470 and so on, only can give out noise of several frequency points or of several fixed frequency, no more give out two pat meters. Thus it can be seen that if one want to understand all-sidelly the low-frequency noise performance of a semiconductor device, to make researches on semiconductor noise mechanism and to apply low-frequency noise to analyzing the inherent defect of a device and its reliability and so forth, one must make study of the measurement of low-frequency noise spectrum and the computation of its parameters. This important work is absolutely necessary to understand noise performance of a device or a circuit and specially to develop low-noise devices.

In this part, the noise equivalent circuit of OCDs have been analyzed; then noise spectrum measurement systems of OCDs based on FFT analyzer (CF-920, made in Japan) and virtual instrument are presented, their measuring range is 0. 25Hz- l00kHz and accuracy is higher than 4%. Moreover, the white noise level and corner frequency are computed by applying weighed least square method.

3.1 The noise equivalent circuit of OCDs

Fig. 2 shows the schematic diagram of the OCDs circuit. The OCDs measured and analyzed in this paper are GD315A, made in China. It is well known that if the input current I_0 of a laser diode is less than the threshold current I_{ph}, the noise equivalent circuit of a

semiconductor laser diode can also be used to explain the noise performance of an LED. Fig. 3 shows the noise equivalent circuit of OCDs. It is composed of LED and optotransistor shown in the left portion and the right one, respectively. Where R_s is the source resistance, i_{Rs} is the thermal noise of R_s. The quantities in and v_n are the intrinsic noise sources of LED, the sources in and v_n are partially correlated due to the coupled rates. Their noise spectral densities are shown as follows:

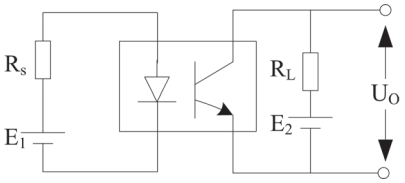

Fig. 2. The schematic diagram of OCDs.

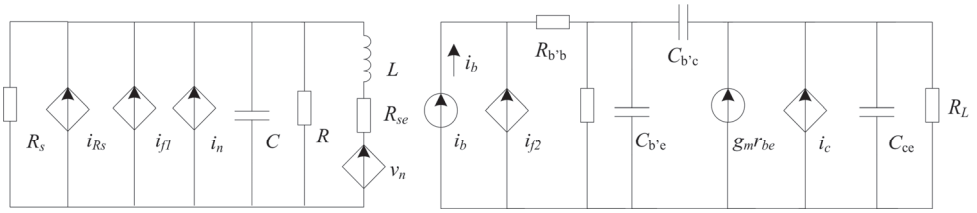

Fig. 3. The noise equivalent circuit of OCDs.

$$S_{i_n}(f) = 2qi_0 + 4q^2 E_{vc} S_0 \tag{4}$$

$$S_{v_n}(f) = \frac{4(mV_T)^2}{(n_0(AS_0 + (\beta/\tau_s)))^2} \frac{1}{\tau_{ph}} + E_{vc} S_0 \tag{5}$$

$$S_{v_n i_n}(f) = 2\frac{mV_T q}{n_0(AS_0 + \beta/\tau_s)} \frac{1}{\tau_{ph} + 2E_{vc}} S_0 \tag{6}$$

The current i_{f1} denotes the low frequency noise source in LED. The definition of all symbols in Eqs. (4) - (6) and circuit parameters R, C, L, R_{se} in the LED equivalent circuit in Fig. 3 can be found in the references and another publication. In the noise equivalent circuit of the phototransistor, i_b is the base noise current, it is caused by the noise current i_L in LED, hence i_b can be written as γi_L, where γ can be calculated by the current transfer ratio (CTR) of OCDs. Since CTR is defined as I_c/I_0, in the low frequency region all capacitors in the OCDs are omitted; from Fig. 3 we have

$$CTR = \frac{I_c}{I_0} = \frac{\gamma g_m R_L R_{se}(r_{b'b} + r_{be})}{(R + R_{se})(R_L + R_{ce})} \tag{7}$$

Then γ can be calculated by Eq. (7). In the high frequency region, CTR will decrease due to the influence of circuit capacitance. The CTR of OCDs can be obtained by measurement of OCDs (GD315A) as is shown in Fig. 4, where curve 1 is measured in the condition R_L=1kΩ, and curve 2 is R_L=500Ω.

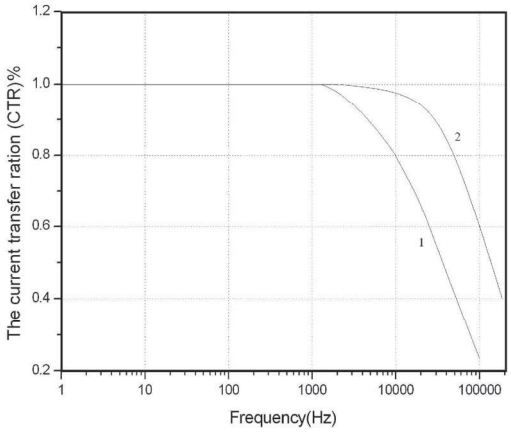

Fig. 4. The CTR of OCDs versus frequency.

In the equivalent circuit of the phototransistor, i_{f2} denotes the low frequency noise source in it. $r_{b'b}$, r_{be}, g_m, $C_{b'e}$, C_{bc}, C_{ce} are the circuit parameters of phototransistor shown in Fig. 3.

3.2 Noise spectrum measurement systems

3.2.1 Noise measurement system based on FFT analyzer

Fig. 5 is the measurement system block scheme of low-frequency noise spectrum testing system we have developed. In our experiments, a dual-channel low frequency amplifier (LNA) chain and the CF-920 cross-spectrum estimator have been used to reduce the background noise of measurement system; hence the noise in the amplifiers will not contribute to the cross-spectrum measured by this system. Therefore, the output voltage noise spectrum of OCDs can be written as

$$S_0(\omega) = \frac{S(\omega)}{K_1 K_2} \tag{8}$$

Where S(ω) is the cross-spectrum measured by CF-920, K_1 and K_2 are the gains of the dual-channel amplifiers LNA I and LNA II, respectively.

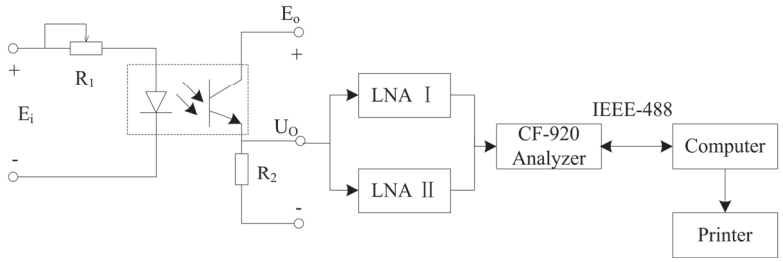

Fig. 5. The noise measurement system of OCDs using CF-920.

In the testing system, the cross-spectrum density estimation method was used to reduce the noise contribution of two preamplifiers. The reason was that two sets of batteries were used as the power supplies for the preamplifiers so that the noises in the two preamplifiers

themselves were uncorrelated. So, the measuring system can be used to measure a much smaller signal than usual.
Thus it can be seen that amplifier's self-measurement error has been eliminated basically according to the measuring method in this system. And the measurement accuracy of noise spectrum is mainly decided by CF-920. The measuring range of this system is 0. 25 Hz-100 KHz frequency wide and accuracy is higher than 4%. In the whole measurement process, the measurement and the output of measuring results are controlled automatically by computer.

3.2.2 Noise measurement system based on virtual instrument

Considering the large volume of CF-920 in the above system, which is inconvenient to carry, we design a new measurement system with virtual instrument made by the company of National Instrument and the system block diagram is shown in Fig. 6. It is well known that the virtual instrument platform is widely used in the fields of measurement, auto-control, signal processing and so on, and what the most important is the high precise and small volume.

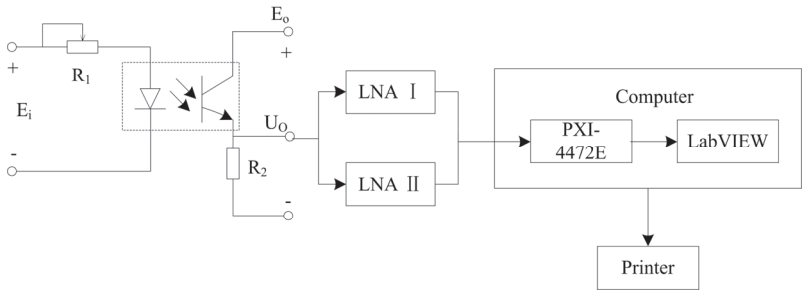

Fig. 6. The noise measurement system of OCDs built on virtual instrument platform.

Where, PXI-4472E is a high-precision 24-bit data acquisition card which acquires the signal from the preamplifiers. The noise signals could be processed for cross-spectral transform, components of noise spectrum estimation and the noise spectrum analysis algorithm in a software developed in LabVIEW. The equivalent input noise power spectrum as Eq. (9) can be tested through low-frequency noise spectrum measurement system.

$$S(f) = A + \frac{B}{f^{\alpha}} + \sum_{i=1}^{N} \frac{\frac{C_i}{f_{oi}}}{1 + (\frac{f}{f_{oi}})^2} \tag{9}$$

Where A, B and C_i are amplitudes of white noise, 1/f noise and G-R noise respectively; α is a constant 1; f_{oi} is the corner frequency of excess G-R noise; N is the number of G-R noise sources in devices. As long as parameters A, B and C_i are estimated, the magnitude of each type of noise in the device can be determined. A genetic algorithm which would be discussed below was used to fit the parameters, so the coefficient of white noise, 1/f noise and G-R noise were obtained quickly and accurately across the entire spectrum.

3.2.3 Noise analysis of OCDs

According to the noise equivalent circuit given in Fig.3, the noise curves are analyzed in various frequency ranges.

(1) *Low frequency range (1 Hz < f <1 kHz)*: In this frequency range, the 1/f noise and generation-recombination g-r noise are dominant. We measured the noise spectrum of 205 OCDs (GD315A made in China), the noise spectrum for four typical devices are shown in Fig. 7. These devices exhibit various low frequency noises. Using the curve fitting method, the analysis results of noise spectrum for four typical devices shown in Fig. 7 are given as follows:

$$\text{NO.4}\quad S_0(f) = 5\times10^{-13} + \frac{0.85\times10^{-10}}{\mathrm{f}} + \frac{0.014\times10^{-10}}{1+(\mathrm{f}/15)^2} V^2/Hz$$

$$\text{NO.45}\quad S_0(f) = 2\times10^{-13} + \frac{4\times10^{-10}}{\mathrm{f}} + \frac{0.07\times10^{-10}}{1+(\mathrm{f}/15)^2} V^2/Hz$$

$$\text{NO.102}\quad S_0(f) = 1.05\times10^{-13} + \frac{1\times10^{-10}}{\mathrm{f}} + \frac{2.13\times10^{-10}}{1+(\mathrm{f}/15)^2} V^2/Hz$$

$$\text{NO.15}\quad S_0(f) = 8\times10^{-13} + \frac{6.28\times10^{-10}}{\mathrm{f}} + \frac{0.64\times10^{-7}}{1+(\mathrm{f}/2500)^2} V^2/Hz$$

The noise analysis results show that OCD No. 4 exhibits a normal low frequency noise, No. 45 has excess 1/f noise, No. 102 has excess g-r noise (the corner frequency is 15 Hz), and No. 15 has excess 1/f noise and g-r noise with burst noise waveform. It means that OCDs No. 4 is a reliable device, No. 45, 102 and 15 coincide with various defects in OCDs, and i.e. their quality is poor.

(2) *Medium frequency range (1 kHz < f <10 kHz)*: In this frequency range, the low frequency noise current i_{f1} and i_{f2} in the OCDs can be omitted; hence, the OCDs output noise is caused by shot noise $i_c(t)$, thermal noise $i_{Rs}(t)$ and the spontaneous emission noise i_n and v_n. Omitting all capacitors in the OCDs, the output noise spectrum can be obtained:

$$S_0(\omega) = R_L^2(CTR)^2\left(S_{i_{Rs}}(\omega) + S_{i_n}(\omega) + \frac{S_{v_n}(\omega)}{R_{se}^2} + \frac{2S_{i_n v_n}(\omega)}{R_{se}}\right) + R_L^2 S_{ic}(\omega) \tag{10}$$

Where $S_{iRs}=4kT/R_s$, $S_{ic}(\omega)=2qI_c$. According to the Reference written by Harder C et al, the noise current source i_n in parallel with the junction represents mainly the fluctuation in electron population. The first term on the right-hand side of Eq. (4) is the usual shot noise term $2qI_0$ of OCDs, the second term results from the fact that the noise is determined by the sum of emission and absorption. The noise voltage source v_n results from the fluctuation of the photon population.

Since the input current I_0 of LED is less than the threshold current I_{ph}, if we omit the second term of in and v_n, Eq. (11) can be written as follows:

$$S_0(\omega) = 2qI_0CTR^2R_L^2 + 2qI_0R_L^2 \tag{11}$$

Let I_0=10mA, CTR=1, R_L=390Ω, R_s=360Ω, I_c=10mA, from Eq. (11) we obtain the output noise voltage spectrum $S_0(\omega)=9.7\times10^{-16}V^2/Hz$. The effective value of $S_0(\omega)$ equals $31.2\,nV/\sqrt{Hz}$ which is smaller than the measurement result ($287\text{-}488\,nV/\sqrt{Hz}$). It means that the second term of i_n and v_n caused by the spontaneous emission in LED cannot be omitted.

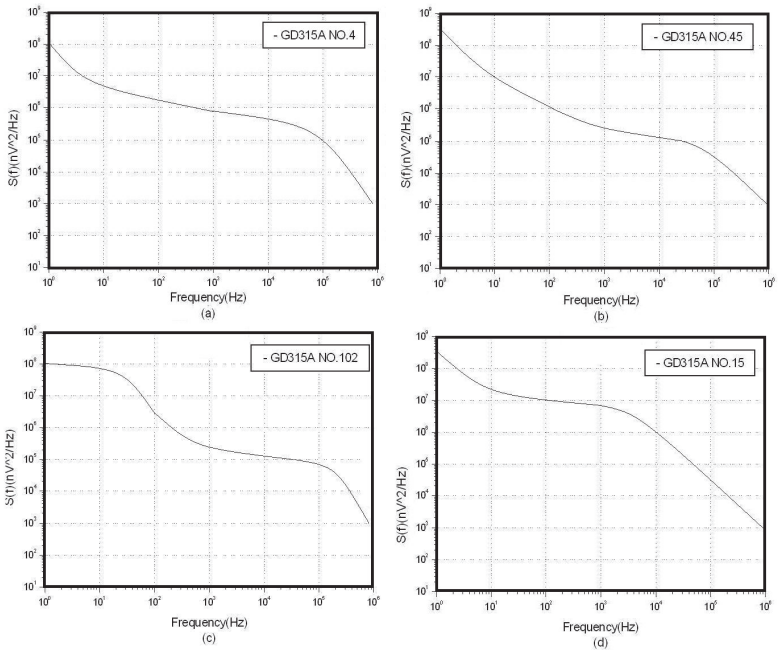

Fig. 7. The noise measurement system of OCDs built on virtual instrument platform.

(3) *High frequency range (10 kHz < f <100 kHz)*: In this frequency range, the white noise is dominant, so that the output noise spectrum of the OCDs is a flat form. However, the noise measurement for 205 OCDs (DG315A) shows that the noise spectrum of all OCDs decreases from 10 to 100 kHz, as shown in Fig. 7. It can be explained as follows: Since $S_0(\omega)$ is directly proportional to CTR2 (Eq. (11)) and CTR decreases from 10 to 100 kHz (Fig. 4), as a consequence, the decrease in noise spectrums of OCDs is caused by the decrease of CTR. Because all capacitors in the OCDs will influence the output noise in this frequency range, the decrease of CTR seems to obey the circuit response.

4. Discussion of the optical screening criterion for OCDs

Generally, it has been already accepted that 1/f noise is closely related to the surface states of the semiconductor device, g–r noise is related to device bulk defects such as impurities, dislocation, and burst noise is related to lattice dislocation as well as heavy metal impurity deposits. From the generation mechanisms of 1/f, g–r and burst noise, it can be seen that the probability to generate these three types of noise by the same defect is quite small although some defects may cause more than one of them simultaneously in some cases.

Hence, in order to exclude these defects and meet high reliability, we can use the three independent noises, 1/f, g–r and burst noise, as reliability indicators for quality estimation of OCDs. In this way even if some defects can cause two or three of them at the same time, such as emitter region edge dislocation which makes both 1/f noise and burst noise increase at the same time in most cases, can also be rejected.

Therefore, because an excess noise is closely associated with some defects in the devices and/or imperfections of technology, noise measurement amplitudes can be used to indicate

the defects. In practice, we found that the device with burst noise can be found from its instantaneous waveform in the time domain. The device with g–r noise can be found through noise component analysis or ratio of noise value at 10 Hz to noise value at 1 Hz (which will be explained and proved in later part), which is used to judge whether there is g–r noise or not. And the device with 1/f noise can be judged by the amplitude of voltage noise value at 1 Hz

Therefore, it is necessary that there be three independent screening conditions to meet the requirement of high reliability to reject the devices with excess 1/f, g–r or burst noise. We take the OCDs of GD315A as an example to present the conditions which are presented as follows.

(1) *The value of the noise spectrum at 1 Hz*: Since 1/f noise depends on the surface and bulk defects in OCDs, and it is dominant in the low frequency region, we select the effective value U_0 of noise spectrum at 1 Hz as the reliability indicator. Fig. 8 shows the histogram of the effective value U_0 of 205 OCDs. We can see that the U_0 of most of OCDs obeys the normal distribution; it can be explained by the discretion of OCDs parameters. However, a few of OCDs exhibit excess 1/f noise, it means that these OCDs may contain surface or bulk defects (such as crystal defects and contamination, emitter edge dislocations, electromigration, imperfection of chip bonding, etc.); hence, they should be recognized as poor quality devices.

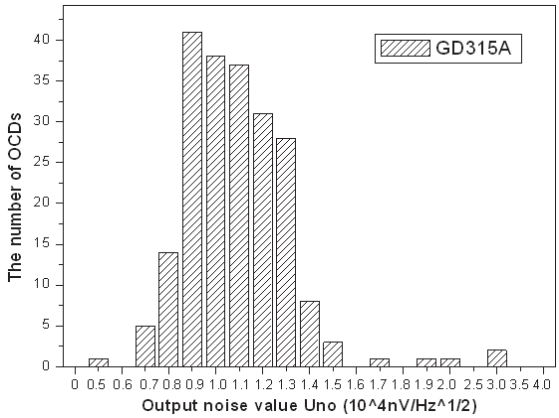

Fig. 8. The histogram of the output noise value $S_0(f)$ of 205 OCDs.

Konczakowska suggested a classification algorithm which has been verified by reliability experiments. On the basis of noise measurement results, we can classify quality groups according to this rule. At first, the mean value and variance of U_0 for 205 OCDs have been calculated, and then the border values for quality groups (i.e., the threshold value) are

$$U_{01} = \bar{U}_0 - \alpha\sigma$$

$$U_{02} = \bar{U}_0 + \alpha\sigma$$

where $\bar{U}_0$ denotes the mean value of U_0, r denotes the variance of U0 and a equals 0.67. In our experiment, the statistical results are $\bar{U}_0 = 11467.5nV/\sqrt{Hz}$, $\sigma = 3194nV/\sqrt{Hz}$, then

we obtain $\bar{U}_{01} = 9327.4nV/\sqrt{Hz}$, $\bar{U}_{02} = 13607.7nV/\sqrt{Hz}$. The value of classifying OCDs into three groups according to the 1/f noise is as follows:

- first group $-U_0 \le 9327.4nV/\sqrt{Hz}$, high quality is expected;
- second group $-9327.4\text{nV}/\sqrt{\text{Hz}} \le U_0 \le 13607.7nV/\sqrt{Hz}$, good quality is expected;
- third group $-U_0 \ge 13607.7nV/\sqrt{Hz}$, poor quality is expected.

(2) *The ratio of noise spectrum at 10 and 1 Hz*: The g-r noise is caused by the defects in the crystal structure of devices and the deep-level impurity in the p-n junction; hence the g-r noise is used as one of the noise reliability indicators. The g-r noise in OCDs can be separated accurately from the output noise spectrum using the curve fitting method; however, it must take a long time and is not suitable for practical application. For the convenience of direct industrial application, we suggest the g-r noise indicator as follows:

$$r = \frac{U_0(f_0)}{U_0(1Hz)} \tag{12}$$

where U_0(1 Hz) is the effective value of noise spectrum at 1 Hz, $U_0(f_0)$ is one at the corner frequency f_0 of g-r noise. From the noise measurement of OCDs, we found that the corner frequency of most OCDs is about 10 Hz, hence we can select f_0=10 Hz.

If the output noise spectrum consists of only white noise and 1/f noise, in the low frequency region, we have

$$S_0(f) = A + \frac{B}{f} \tag{13}$$

If the 1/f noise is dominant, then $S_0(f)=B/f$, the value of r equals $U_0(10Hz)/U_0(1Hz) = 1/\sqrt{10} = 0.33$. If the white noise is dominant, r=0, so that the value of r is in the range of 0-0.33. However, if an OCD exhibits g-r noise, the noise spectrum is shown in a platform below the corner frequency f_0. As a consequence, the value of r is greater than 0.33. In Fig. 9, the histogram of the value r for 205 OCDs is shown. We can see that the value of r for most of the OCDs obeys the normal distribution. The statistical results from 205 GD315A are $\bar{r} = 0.36$ and $\sigma_r = 0.16$. If we select the value of β equal 2, then the threshold value of r is

$$r = \bar{r} + \beta\sigma_r = 0.68$$

The rule of classifying OCDs into two groups according to the g-r noise is as follows:

- r < 0.68, first group, high quality is expected;
- r > 0.68, second group, poor quality is expected.

(3) *Burst noise in OCDs*: A number of experiments have already shown that heavy metal impurity deposits and lattice dislocations are the major sources of burst noise for a transistor or IC, so that OCDs with burst noise should always be rejected in any case, because it cannot only effect device reliability, but also hinder the normal operation, especially in digital circuit.

The rule of classifying OCDs into two groups according to the burst noise is as follows:

- no burst noise: first group, high quality is expected;
- with burst noise: second group, poor quality is expected.

As a result, the reliability screening conditions of OCDs are

1. $U_0(1Hz) \geq 13607.7nV / \sqrt{Hz}$
2. $r \geq 0.68$
3. with burst noise

The device will be rejected if it meets any condition of the three. The result of the noise measurement for 205 OCDs is that 23 OCDs are rejected by our reliability screening conditions. Among these OCDs, 19 OCDs are rejected by reliability screening condition 1 (here two OCDs exhibit burst noise). Four OCDs are rejected by condition 2 (here one OCD exhibits burst noise).

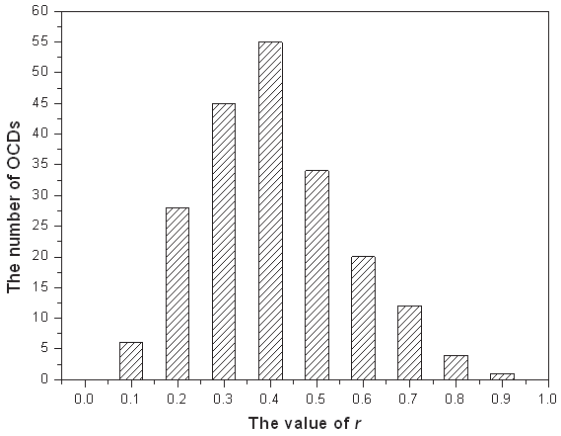

Fig. 9. The histogram of value *r* of 205 OCDs.

5. Conclusion

In this paper, we analyzed the noise performance of OCDs using the noise equivalent circuit of LED and bipolar transistor.

(1) In the low frequency region (f <1 Hz), the excess 1/f noise and g-r noise can be used as noise reliability indicators; then three reliability indicators have been suggested for quality and reliability screening of OCDs, which have the advantages of general and convenience for direct industrial application.

(2) In the medium frequency region (1 kHz < f <10 kHz), the output noise measurement results show that the fluctuation of the photon population (emission and absorption) in OCDs must be considered. Hence, the value of output noise is larger than usual shot noise in transistor.

(3) In the high frequency region (f > 10 kHz), the output noise will decrease due to the decrease of the current transfer ratio (CTR) of OCDs in this frequency region.

Then the 205 OCDs have been measured by the low noise measurement systems which have high reliability and the satisfactory accuracy. The screening thresholds and experimental results are given. Based on the results, it can be obtained as follows:

(1) It can be found that 1/f noise, g–r noise and burst noise must be used as three independent noise criteria for high reliability estimation.

(2) It is necessary that the estimated error and the maximum value of failure ratio r should be considered together in order to obtain optimal noise thresholds.

(3) In this paper the ratio of Vn(10 Hz) to Vn(1 Hz) was chosen as a screening threshold instead of g–r noise component analysis of noise spectrum, for this reliability indicator is more simple and convenient than the calculation of g–r noise component, especially during the practical screening of a large number of devices.

6. Acknowledgment

Dr. Qiuzhan Zhou would pay the highest respect to his advisor, Prof. Dai Yisong and would like to thank for Prof. Dai's patient guide since 1998. The authors would also thank Prof. Zhang Xinfa for his help on noise parameters measurement. This work is part of Project 60906034 supported by National Natural Science Foundation of China and Project 201115029 supported by Provincial Natural Science Foundation of Jilin Province.

7. References

A. Konczakowska(1995), Quality and 1/f noise of electronic components, *Quality and Reliability Engineering International*, vol. 11, pp. 165-169, ISSN 1099-1638

Bernard O & Philippe S & Jean-Marie P et al(1994), Correlation between electrical laser diodes, *IEEE Transactions on Electron Devices*, vol. 41, pp. 2151-2161, ISSN 0018-9383

Dai.Y& Xu. J(2000). The noise analysis and noise reliability indicators of optoelectron coupled devices, *Solid-State Electronics*, vol. 44, pp. 1495-1500, ISSN 0038-1101

Dai.Y(1991), Optimal low frequency noise criteria used as a reliability test for BJTs and their experimental results, *Microelectronics Reliability*, vol. 31, pp. 75-78, ISSN 0026-2714

Dai.Y(1997), A precision noise measurement and analysis method used to estimate reliability of semiconductor devices, *Microelectronics Reliability*, vol. 37, No. 6, pp. 893-899, ISSN 0026-2714/97

Dai.Y(1991), The performance analysis of cross-spectral density estimator and its applications, *International Journal of Electronics*, vol. 71, pp. 45-53, ISSN 0020-7217

Doru U, Jones BK(1996), Low frequency noise used as a lifetime test of LEDs, *Semiconductor Science and Technology*, vol. 11, pp. 1133-1136, ISSN 0268-1242

Harder C & Katz J & Margalit S et al(1982), Noise equivalent circuit of a semiconductor laser diode, *IEEE J Quant Electron*, vol. 18, pp. 333-337, ISSN 0018-9197

Lei. N,& Du.J & Zhou. Q Z (2009), Fitting Noise Power Spectrum Parameters by Squared Distance Minimization, *Computational Intelligence and Software Engineering, 2009.* pp. 1-4. ISBN: 978-1-4244-4507-3

Levinzon, F. A.(2005), Measurement of low-frequency noise of modern low-noise junction field effect transistors, *Instrumentation and Measurement, IEEE Transactions on*,Vol.54,pp.2427-2432,ISSN 0018-9456

M.M. Jevtic(1995), Noise as a diagnostic and prediction tool in reliability physics, *Microelectronics Reliability*, vol.35, pp. 455-477, ISSN 0026-2714/97

Vandamme L. K. J (1994), Noise as a diagnostic tool for quality and reliability of electronic devices, *Electron Devices, IEEE Transactions on*, vol. 41, pp. 2176-2187, ISSN 0018-9383

Wu,D E &Zhou Q Z &Liu P P(2009) Study of OCDs Reliability Estimation System Based on Bio-Immunology, *Journal of Bionic Engineering*, vol. 6, pp. 306-310, ISSN 1672-6529

Xu.J & Abbott.D & Dai. Y (2000), 1/f, g-r and burst noise used as a screening threshold for reliability estimation of optoelectronic coupled devices, *Microelectronics Reliability*, vol. 40, pp. 171-178, ISSN 0026-2714

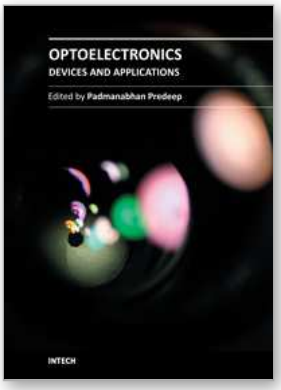

Optoelectronics - Devices and Applications

Edited by Prof. P. Predeep

ISBN 978-953-307-576-1
Hard cover, 630 pages
Publisher InTech
Published online 03, October, 2011
Published in print edition October, 2011

Optoelectronics - Devices and Applications is the second part of an edited anthology on the multifaced areas of optoelectronics by a selected group of authors including promising novices to experts in the field. Photonics and optoelectronics are making an impact multiple times as the semiconductor revolution made on the quality of our life. In telecommunication, entertainment devices, computational techniques, clean energy harvesting, medical instrumentation, materials and device characterization and scores of other areas of R&D the science of optics and electronics get coupled by fine technology advances to make incredibly large strides. The technology of light has advanced to a stage where disciplines sans boundaries are finding it indispensable. New design concepts are fast emerging and being tested and applications developed in an unimaginable pace and speed. The wide spectrum of topics related to optoelectronics and photonics presented here is sure to make this collection of essays extremely useful to students and other stake holders in the field such as researchers and device designers.

InTech Europe
University Campus STeP Ri
Slavka Krautzeka 83/A
51000 Rijeka, Croatia
Phone: +385 (51) 770 447
Fax: +385 (51) 686 166
www.intechopen.com

InTech China
Unit 405, Office Block, Hotel Equatorial Shanghai
No.65, Yan An Road (West), Shanghai, 200040, China
中国上海市延安西路65号上海国际贵都大饭店办公楼405单元
Phone: +86-21-62489820
Fax: +86-21-62489821